CHAPTER IV
PREPARATION AND CHARACTERIZATION OF BACTERIAL CELLULOSE/POLY(VINYLIDENE FLUORIDE) BLEND FILMS

4.1 Abstract

The bio-based piezoelectric blend films were prepared from the bacterial cellulose (BC) and poly(vinylidene fluoride) (PVDF) at various weight compositions (BC/PVDF: 0/100, 2.5/97.5, 5/95, 10/90 and 15/85). The blend films were successfully fabricated via two steps: (1) solution casting and (2) hot-pressing. The intermolecular interaction between hydroxyl group of BC and fluorine atom of PVDF chain had influenced to crystalline phase behavior, thermal, mechanical, optical and dielectric properties of blend films. The mixed phase crystallinity and slight increase of thermal stability were obtained. The higher storage modulus and dielectric properties were observed when BC was incorporated in the blend but not the transparency.

4.2 Introduction

In the last decade, touchscreen has been one of the most popular technologies for electronic devices (Shin *et al.*, 2013). Several applications such as smart phone, tablet, smart watch are required this technology. Piezoelectric touch sensor, the unpopular touch technology was introduced to overcome the limitations of common touch technology by combined the benefits of both capacitive and resistive touch sensors. Similar to resistive screen, piezoelectric materials can respond to both of charged and uncharged objects. In addition, this piezoelectric touch sensor has high sensitivity and can be used as multi-touching as capacitive touchscreen. Moreover, it has ability to generate and accumulate the electrical power by mechanical energy without using external battery (O-Rak, 2013).

Poly(vinylidene fluoride), (PVDF) become the interest for electronic devices such as sensor, actuator, transducer, etc. The reason why using this due to its

advantages of high dielectric, high piezoelectric properties compared to other polymeric materials, flexibility and processability compared to ceramic materials (Harrison *et al.*, 2001). PVDF is the polymeric material that has several types of crystal morphologies. The most common phase of PVDF is α-phase crystal , that's thermodynamically stabilized phase and can be obtained from melt processing. but the origin of piezoelectric properties is β-phase crystal. β-phase crystal has TTTT (all-trans, planar zigzag) conformation structure that exhibits the high dipole moment. while α-phase crystal has $TG^{+}TG^{-}$ conformations structure that exhibits almost zero of net dipole moment (Fukada *et al.*, 1981).

Due to the petrochemical-based materials caused the environmental problems and the global warming effect (Ratanakamnuana *et al.*, 2012). Achievement of this novel promising concept can easily offer numerous potential applications. Bacterial cellulose (BC) is a biopolymer that can be produced from *Acetobacter Xylinum* (Shah *et al.*, 2013; Wu *et al.*, 2014). It has nano-sized extracellular network structure and also unique properties such as high mechanical strength, high crystallinity (Tang *et al.*, 2008).

The objective of this research is to prepare the bio-piezoelectric blend from the bio-based BC and piezoelectric PVDF. The effect of BC in BC/PVDF blend films on crystalline phase, morphological, thermal, mechanical, optical and dielectric properties of the blend films were discussed.

4.3 Experimental Procedures

4.3.1 Materials

Nata de coco was purchased from local food market. Poly(vinylidene fluoride) (PVDF) (SOLEF1008) was kindly supported by Solvay (Thailand) Co., Ltd. N,N-dimethylformamide (DMF) (AR grade, 99.8%) and sodium hydroxide (NaOH) (AR grade, 98%) were purchased from RCI labscan Co., Ltd. and Merck Ltd., respectively.

4.3.2 BC Preparation (Maneerung *et al.*, 2008)

Nata de coco gel was firstly washed with water to remove some excess sugar. After that the washed nata de coco gel was grinded and treated with 0.1 M NaOH at 80 °C for 1 h to obtain the BC pellicles. The BC pellicles were then washed with hot deionized water until neutral pH is reached. The BC pellicles were dispersed in deionized water and kept in bottle. Density of BC pellicles would be determined after freeze-drying.

4.3.3 Fabrication of BC/PVDF Blend Films

BC pellicles were rinsed with DMF solution to remove all water content. Then BC pellicles dispersed in DMF solution were obtained. PVDF pellets were dissolved in DMF solution to obtain 10 %wt/v PVDF solution. The obtained solution was further incorporated with BC dispersed in DMF solution with the percentage weight ratio (BC:PVDF) of 0:100, 2.5:97.5, 5:95, 10:90 and 15:85. Then the mixture of BC/PVDF solution was taken into the ultrasonic bath to allow well dispersion for 1 h. Then, the mixture solution was further dropped on clean glass substrates. After that, they were heated in vacuum oven at 80 °C for 3 days, the casted blend films were obtained. Finally, the casted film were performed by a compression press (Labtech, model LP20) with preheating for 20 min, followed by compressing for 45 min at 10 kN. The operating temperature of mould was maintained at 200 °C.

4.3.4 Characterizations

The morphology and dispersion of BC of cross-sectional samples were observed through scanning electron microscope (SEM, TM3000) and transmittance electron microscope (TEM, JEOL-2100). Fourier transform infrared spectroscope (FT-IR, Nicolet, NEXUS 640) and X-rays diffraction microscope (XRD, Rigaku, model Dmax 2002) were used to determine crystalline phases of the films. The thermal properties were investigated by differential scanning calorimeter (DSC, METTLER, DSC822) and thermal gravimetric analyzer (TGA, Perkin Elmer). Tensile properties were investigated follow the ASTM D882. Dynamic mechanical analysis (DMA) was performed in tension mode using a GABO, EPLEXOR 100N at

a constant frequency of 1 Hz to determine dynamic T_g and mechanical relaxation temperature of the blend films. The optical property was determined by using UV/Vis spectrophotometer (Shimadzu 2550). The dielectric constant and dissipation factor were measured using a Network Analyzer (Agilent, E4991A).

4.4 Results and Discussion

4.4.1 BC Characterization

4.4.1.1 Crystallinity of BC

X-ray diffraction pattern of BC sheet prepared from nata de coco was shown in Figure 4.1. The result shows three main diffraction peaks occurring at 14.5°, 16.9° and 22.5° which refer to the 110, 110 and 200 diffraction planes, respectively (Czaja *et al.*, 2004). The result was strongly associated with a crystal lattice of the natural cellulose "cellulose I", which consisted of two crystal structures; a one-chain triclinic structure (I_α) and two-chains monoclinic structure (I_β). In addition, this X-ray diffraction pattern was fitted to DB card number 00-056-1718 which confirms for the presence of cellulose I_β structure.

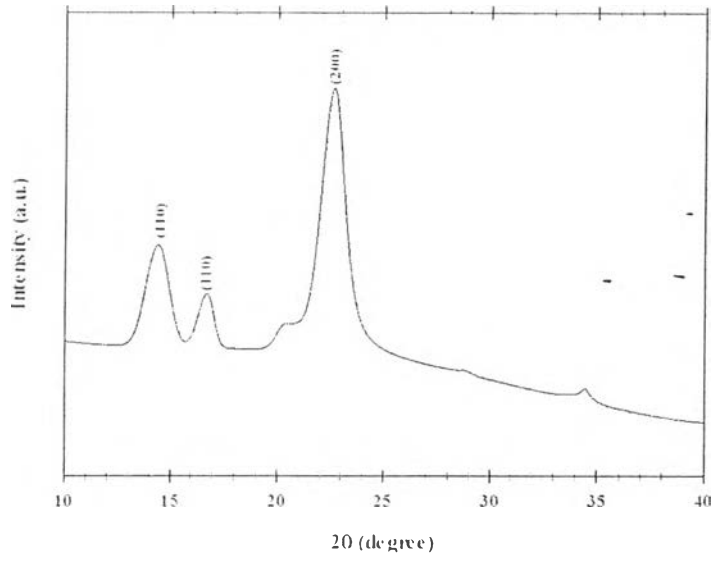

Figure 4.1 X-ray diffraction pattern of BC from nata de coco.

4.4.1.2 Chemical Functionality of BC

The result is shown in Figure 4.2 to confirm that BC was successfully prepared. The structure of cellulose is linear homopolymer composed of D-glucopuranose units linked by β-1,4-glycosidic linkage at C_1 and C_4 carbon position (Ö-Rak, 2013).The peak at 3247 cm^{-1} referred to O-H stretching while at 2980 cm^{-1} and 2860 cm^{-1} referred to C-H stretching of cellulose repeating unit. The peak 1724 cm^{-1} indicated to C=O stretching vibration. At the wavenumber of 1314, 1245, 1152 and 1020 referred to CH_2 rocking at C_6, C-C plus C-O plus C=O stretch, C-O-C asymmetrical stretching, and C-OH , respectively (Halib *et al.*, 2012).

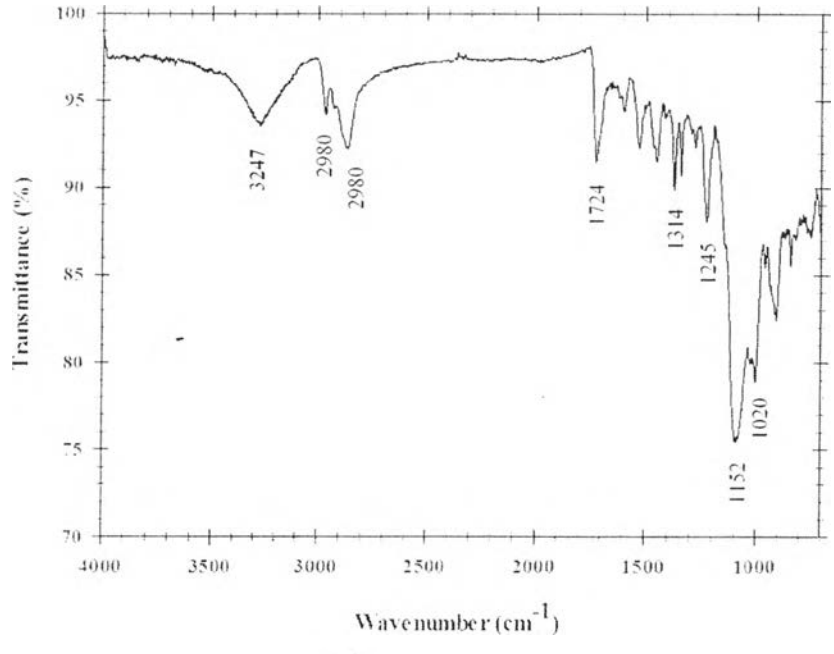

Figure 4.2 FT-IR Spectra of neat BC sheet.

4.4.1.3 Morphological Observation of BC

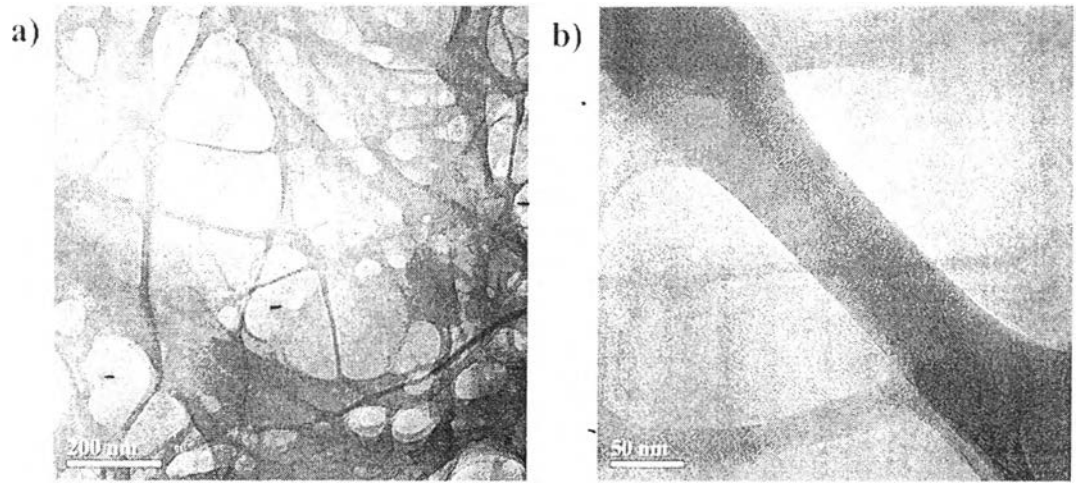

Figure 4.3 TEM images of BC

TEM images show that BC has a network structure as ribbon shaped fibrils with diameter approximately 30-50 nm (Ummartyotin *et al.*, 2012; O-Rak *et al.*, 2014). From Figure 4.3a, due to the network structure, high surface area was obtained which yield to the higher interaction between hydroxyl group of BC surface and polar group in polymer matrix or any filler via physical and chemical attractive forces. Moreover, because of its nano-size the BC was, the higher optical and mechanical properties obtained (Tang *et al.*, 2008).

4.4.1.4 Thermal Properties

Figure 4.4 shows that BC exhibits two thermal degradation steps corresponding to the vaporization of water in the BC (start at 100 °C) and the carbonization and dehydration of BC chain (start at 200 °C). When temperature reaches 450 °C, its thermal behavior becomes stable. At 800 °C, its weight loss was evaluated at approximately 10% referring to char formation (Halib *et al.*, 2012).

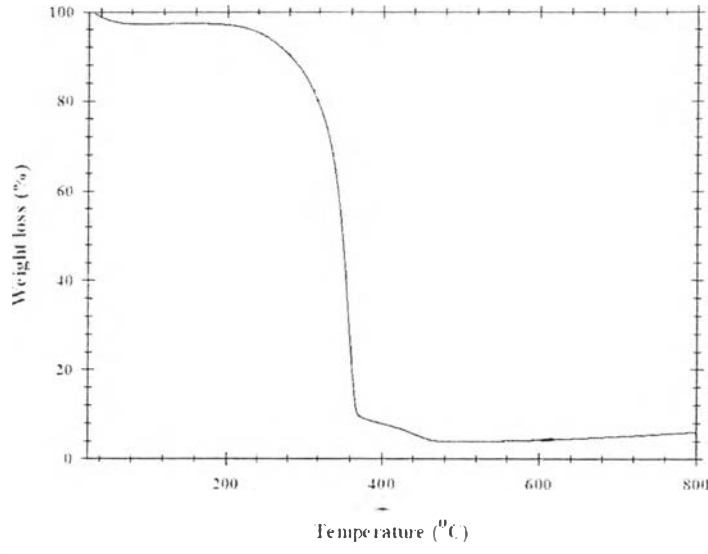

Figure 4.4 TG-DTA thermogram of BC sheet.

As can be seen in the Figure 4.5, there was no any observed from DSC curve in this range. In fact, BC is one type of natural cellulose which has very high amount of crystallinity and very strong hydrogen bonding resulted to the strong attractive force, only the cellulose degradation temperature was observed.

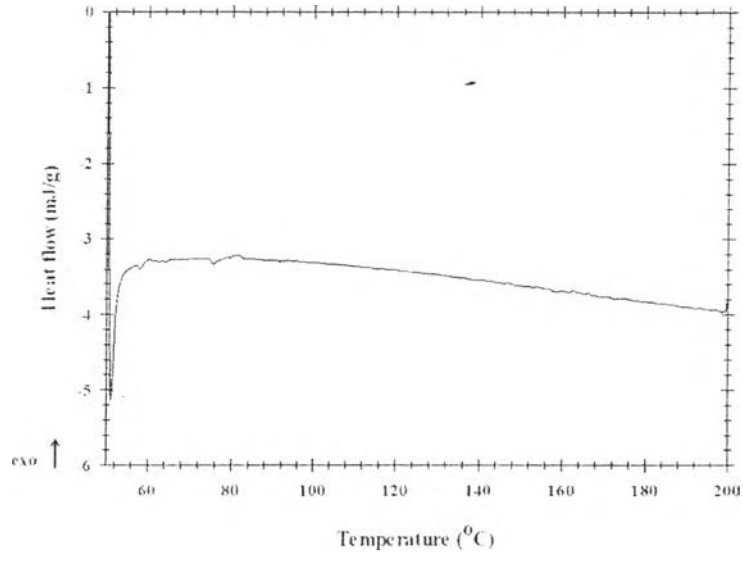

Figure 4.5 DSC curve of BC sheet

4.4.2 BC/PVDF Blend Films Characterization

4.4.2.1 Morphological Properties

Figure 4.6 shows a cross-sectional SEM images of BC/PVDF compared to neat PVDF with the magnification of 10 k. The compressed blend films had no air interstices resulting in smooth surface and higher percent light transmittance (O-Rak, 2013). With the higher amount of BC content, the toughness of the blend film tended to be increased which can be confirmed by the sample's surface fracture. Marcovich *et al.*, (2006) explained that BC can act as rigid fillers which can dissipate the cracking energy causing the different cracking pathways.

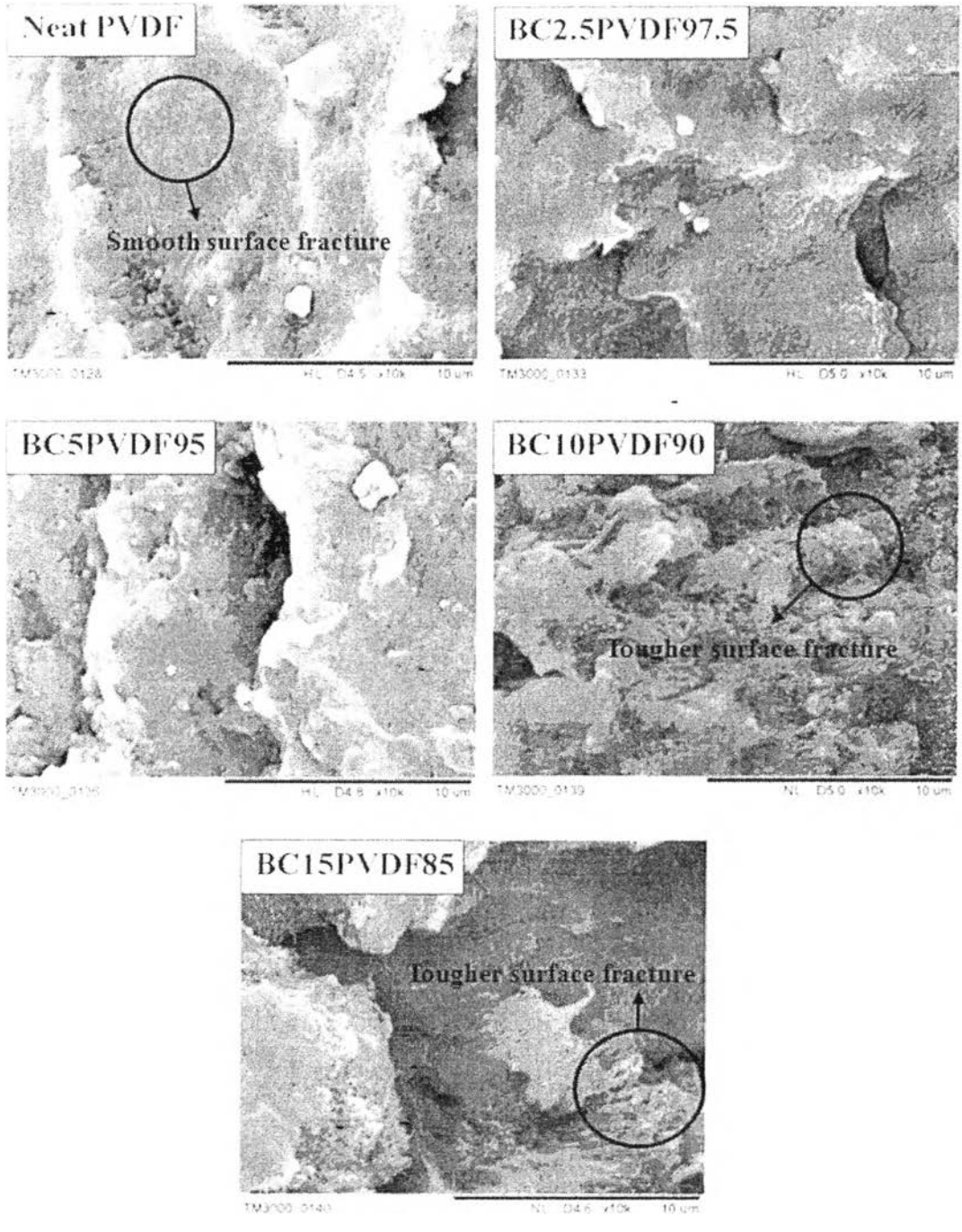

Figure 4.6 SEM images of BC/PVDF blend films at different weight compositions at magnification of 10 k.

4.4.2.2 Crystalline Phase Behavior

In general, the functional group of $-CH_2-CF_2-$ exists five molecular conformations (α, β, δ, γ and ε). In this study, the neat PVDF exhibited two polymorphs; α and β phases as can be seen in Figure 4.7. For the α phase, the vibration bands were observed at 612 cm^{-1}, 763 cm^{-1} (CF_2 bending and skeletal bending), and 795 cm^{-1} (CF_2 rocking) while β-phase, all-trans or planar zigzag conformations, respectively is observed by the presence of specific absorption bands at 840 cm^{-1} (CH_2 rocking) (Salimi *et al.*, 2003; Dahan *et al.*, 2012).

The BC/PVDF blend films also exhibited two polymorphs. Table 4.1 shows that with the higher amount BC incorporated, β phase tends to be increased due to the interaction between hydroxyl groups in BC and fluorine atoms in PVDF which may extend the PVDF chains to all-trans structure. However, when more than 5 wt% of BC was applied, β-crystallinity tends to decrease. This was probably due to the fact that crystallization was obstructed by the network of BC. In addition, the dipole-dipole interaction between the fluorine and oxygen atoms and the amount of β-phase of blend films can affect to their dielectric and piezoelectric properties because of the polarization enhancement. The absorption bands characteristic of neat PVDF and BC/PVDF blend films showed two common polymorphs referred as the α and β phases. Moreover, there is an absence of a peak in the 1630 – 1780 cm^{-1} range which refers to C=O stretching in the DMF molecules. Therefore, it can be noted that both neat PVDF and BC/PVDF blend films can be considered as solvent free.

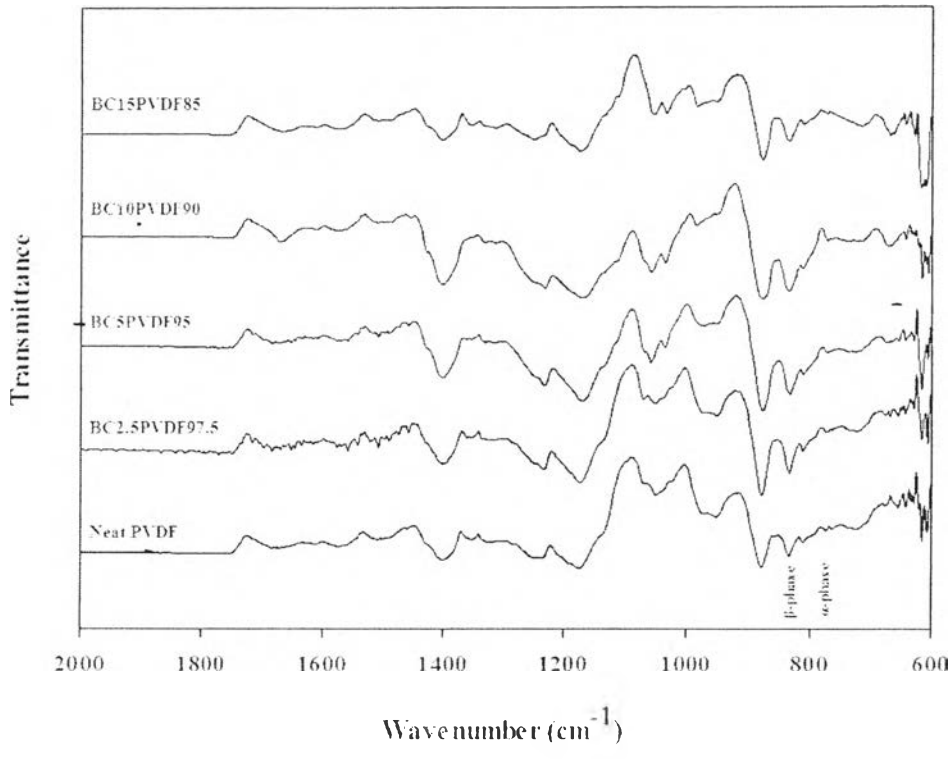

Figure 4.7 FT-IR spectra of BC/PVDF blend films.

Table 4.1 β-phase contents, F(β) of BC/PVDF blend films

Sample	F(β)
Neat PVDF	0.62
BC2.5PVDF97.5	0.64
BC5PVDF5	0.67
BC10PVDF90	0.65
BC15PVDF85	0.57

Figure 4.8 shows XRD patterns of crystalline phase of BC/PVDF blend films with 2.5, 5, 10, and 15 wt% of BC loading compared to neat PVDF. Similar to Chang *et al.*, (2008)s' work, there were two characteristic peaks

which refers to β and α phases. The peaks at 20.4° and 36.7° refer to β phase which has orthorhombic unit cell while the monoclinic α phase can be found at 2θ of 17.9°, 18.6° and 27°. From the XRD result, it was found that neat PVDF has mixed phase of β and α phases which was corresponded to the FT-IR result. When the amount of BC was increased, the β phase tended to increase as can be confirmed by the increasing of the height of diffraction peak at 20.4° and also the decreasing of 18.6° and 27° peak height (Zhang *et al.*, 2012). The height of 20.4° peak tended to decrease when the amount of BC was more than 5 wt%. In addition, when the amount of BC reached 10 wt%, there was a small peak at 22.6° which was corresponded to (200) diffraction plane of BC.

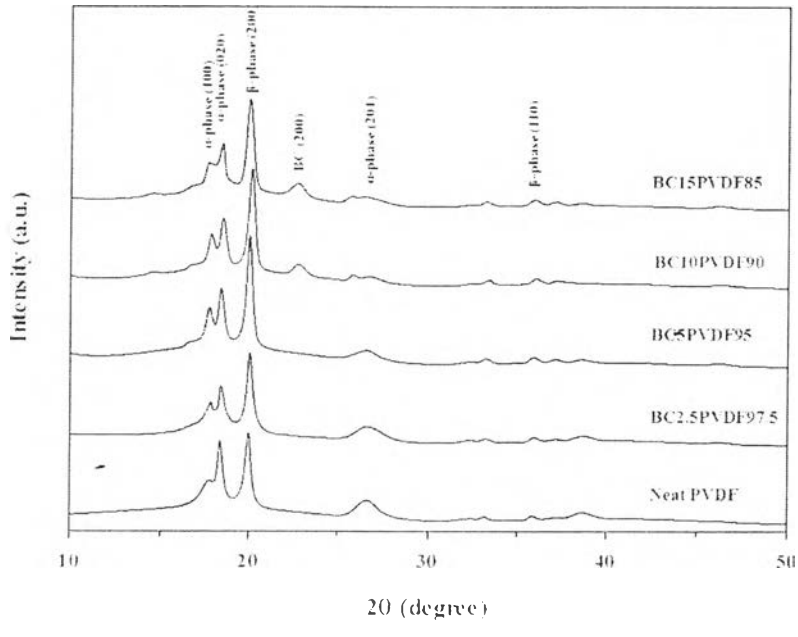

Figure 4.8 X-ray diffraction patterns of BC/PVDF blend films compared to neat PVDF.

4.4.2.3 Thermal Properties

The DSC parameters are shown in Table 4.2. From the result, there was one transition temperature observed at 172 °C and 139 °C which corresponding to T_m and T_c of PVDF.

Figure 4.9 shows the second-heating curves of BC/PVDF blend films. BC has both effects on T_m and PVDF crystallinity (X_C). The results show that increasing of BC content up to 10 wt% can slightly decrease X_C, this occurred because the PVDF crystallization may be disturbed by the nano-fiber network. However, at 15 wt% of BC, X_c tended to increase, this may occur due to agglomeration of BC out of the PVDF matrix resulted in higher possibility of PVDF chains to come close and crystallize (O-Rak, 2013). In addition, there were observed that BC/PVDF blend films had higher T_m than neat PVDF. The reasons why this happened were higher thermal stability of BC and the interaction between hydroxyl groups of BC and fluorine atoms in PVDF chains which was similar to Tang *et al.*, (2008)'s work.

Exothermic peaks of crystallinity temperature are showed in Figure 4.10, indicate that higher amount of BC can shift T_c higher because the blend films need higher energy to crystallize with the presence of BC. Moreover, due to the amount of crystalline in heating step and cooling step were nearly equal, these results can confirm that PVDF crystalline was completely molten.

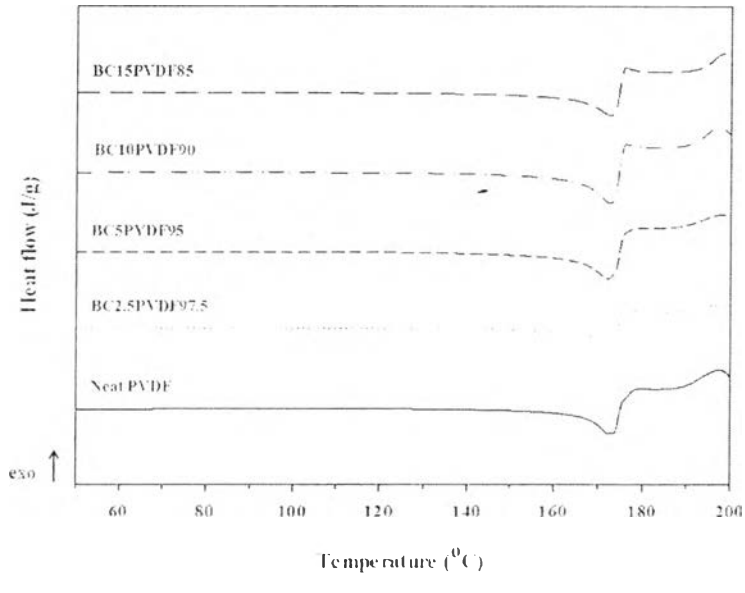

Figure 4.9 DSC second-heating curves of BC/PVDF blend films.

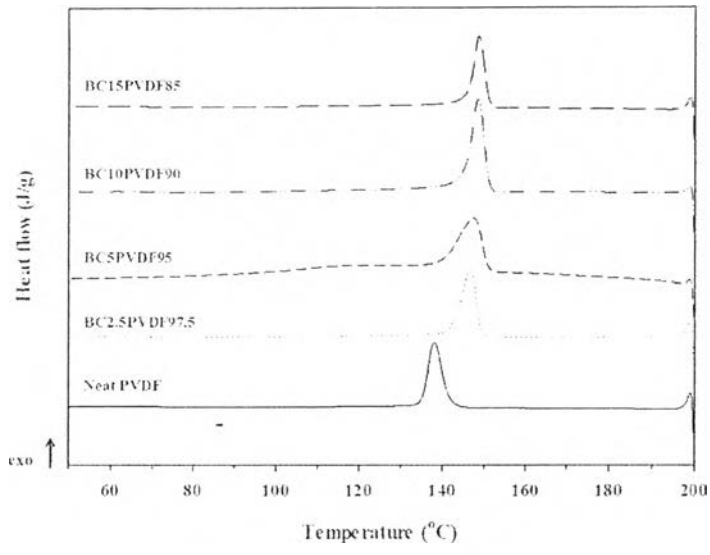

Figure 4.10 DSC first-cooling curves of BC-PVDF blend films.

Table 4.2 DSC parameters of BC/PVDF blend films compared with neat PVDF

Sample	ΔH_m (J/g)	T_m (°C)	X_c (%)	ΔH_c (J/g)	T_c (°C)	X_c (%)
Neat PVDF	45.10	170.7	48.81	45.58	138.5	50.53
BC2.5PVDF97.5	38.55	171.8	42.79	38.61	146.6	43.90
BC5PVDF95	36.72	174.4	41.83	35.18	147.7	41.05
BC10PVDF90	34.57	173.3	41.57	33.08	149.0	40.74
BC15PVDF85	37.49	172.9	47.73	40.25	149.1	52.49

*Heat of fusion value for 100% crystalline PVDF, ΔH_m^o = 92.4 J/g and Heat of crystallization value for 100% crystalline PVDF, ΔH_c^o = 90.2 J/g

Thermal degradation behavior was observed by using TGA. Figure 4.11 shows TGA thermograms of the BC/PVDF blend films. Additionally, a neat PVDF thermogram was provided for comparison. It was found that the thermal degradation behavior of the BC/PVDF blend was divided into two steps. The first step was started at 300 °C, which corresponded to the degradation temperature of BC (Chang *et al.*, 2008). Whereas, the second step, the degradation started at 420 °C,

which corresponded to the degradation temperature of PVDF (Chae *et al.*, 2007). Moreover, it was found that in all BC/PVDF blend films, the degradation temperature was slightly shifted to higher temperature, compared to neat PVDF. It was due to the hydrogen bonds between fluorine atoms in the PVDF main chain and hydroxyl groups in BC (Ummartyotin *et al.*, 2012). Furthermore, it was also found that these BC/PVDF blend films were free from DMF due to the absence of thermal degradation at 150 °C, which was referred to the boiling point of DMF.

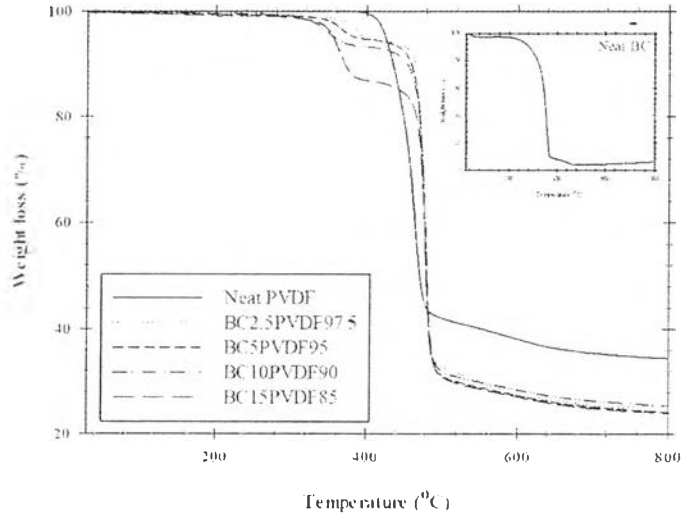

Figure 4.11 TG-DTA thermograms of BC/PVDF blend films.

4.4.2.4 Mechanical Properties

It is noted that BC has extremely higher Young's modulus and tensile strength than PVDF. With the incorporation of BC, the blend films become more ductile as can be seen in Figure 4.12 which corresponded to SEM images in Figure 4.6 that showed the tougher surface fracture. From Figure 4.13, BC provided slightly higher Young's modulus to the blend films compared to neat PVDF. However, it didn't have any effect on the tensile strength of the blend films. From Figure 4.15, it was found that the percentage of elongation at break become increase with the higher amount of BC. This can be explained by the higher amount of amorphous phase and the H-bonds between Fluorine atoms in PVDF chains and hydroxyl group in BC structure which can provide the better interfacial interaction.

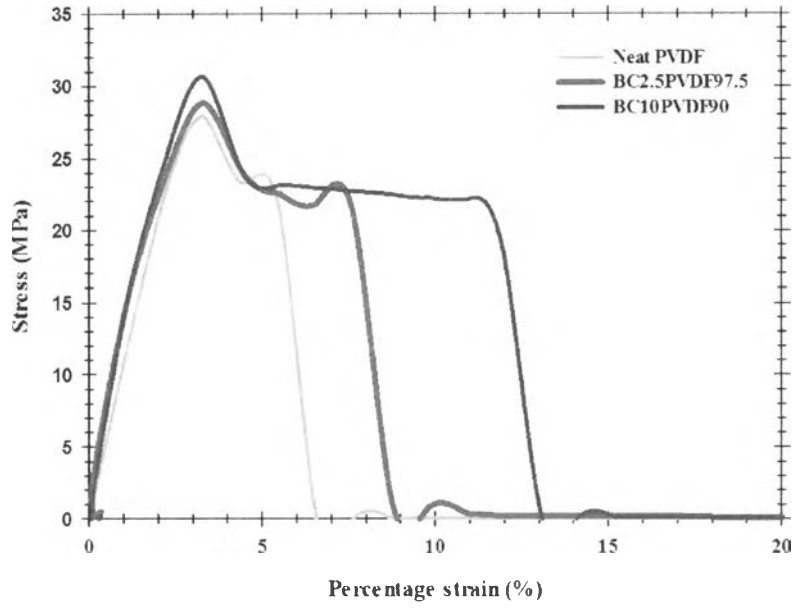

Figure 4.12 Stress-strain curve of BC/PVDF blend films.

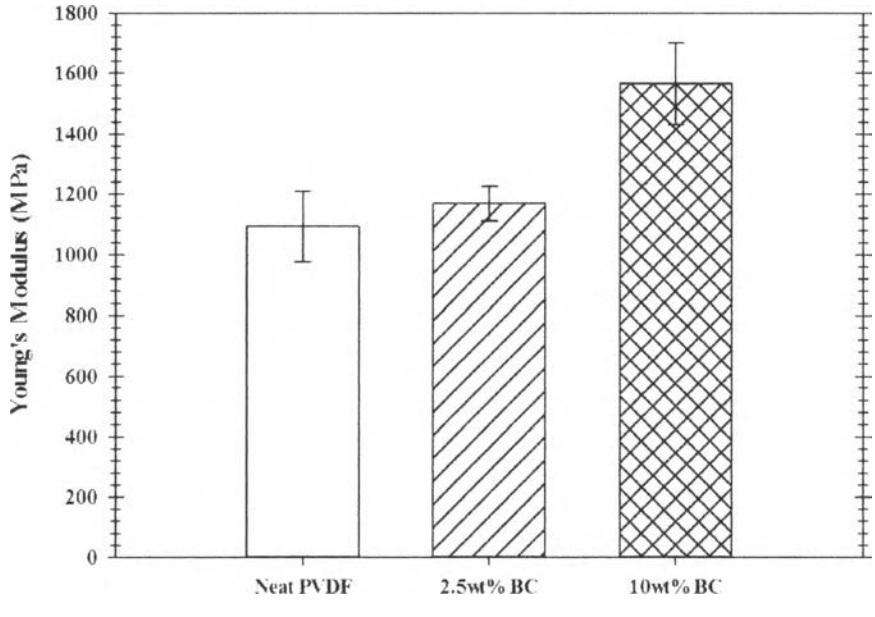

Figure 4.13 Young's modulus of BC/PVDF blend films.

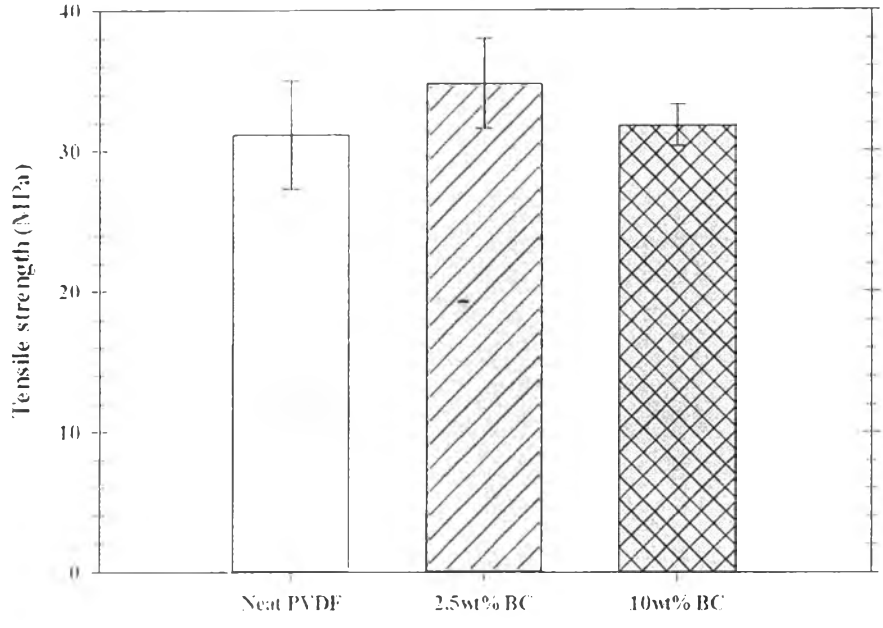

Figure 4.14 Tensile strength of BC/PVDF blend films.

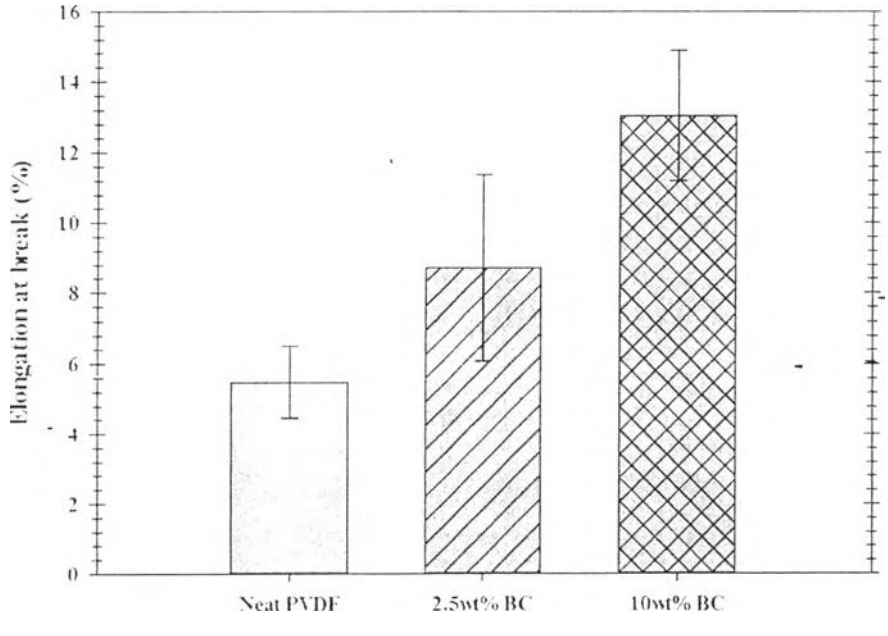

Figure 4.15 Elongation at break of BC/PVDF blend films.

4.4.2.5 Dynamic Mechanical Properties

The dynamic mechanical properties as a function of temperature as various amount of BC in BC/PVDF blend films compared to neat PVDF are shown in Figure 4.16. As the amount of BC increase, the storage modulus also increases. The highest storage modulus was obtained with the incorporation of BC for 15 wt%. With this weight percentage of BC, the storage modulus is also higher than other blend films approximately 1000 MPa throughout the temperature range from -80 °C to 150 °C. At the temperature from -80 °C to -40 °C, incorporated by BC with 10wt% shows the similar storage modulus as 2.5 wt% and 5 wt%, but significantly from -40 °C to 150 °C.

There are three relaxation regions, in the Figure 4.17, these relaxations were referred to β, β' and α relaxation state. The first was called β-relaxation shows the dynamic glass transition temperature (T_g) of material which was found at -40 °C. This relaxation refers to the molecular movement in amorphous regions which referred to the dramatically decreasing of the neat PVDF and its blend films. The second relaxation was found in the temperature range from 0 °C to 50 °C which was referred to β' relaxation. Patro *et al.*, (2008) explained that this relaxation indicated to the folded of amorphous regions due to the compressed-force. The last relaxation called α relaxation that associated with segmental motion in the crystalline regions, exhibited near the melting temperature of PVDF (O-Rak, 2013). The incorporation of BC in the blend films has no effect on the relaxation mechanism of PVDF. However, it was found that the dynamic T_g shifted backwards to lower temperature from -38.7 °C to -46.9 °C with increasing BC content. This can be explained because T_g is only associated with amorphous regions in the PVDF, so the lower amount of PVDF, less energy required to relax and change the state. In addition, BC did not hinder molecular motion of PVDF from glassy state to rubbery state (Rekik *et al.*, 2013).

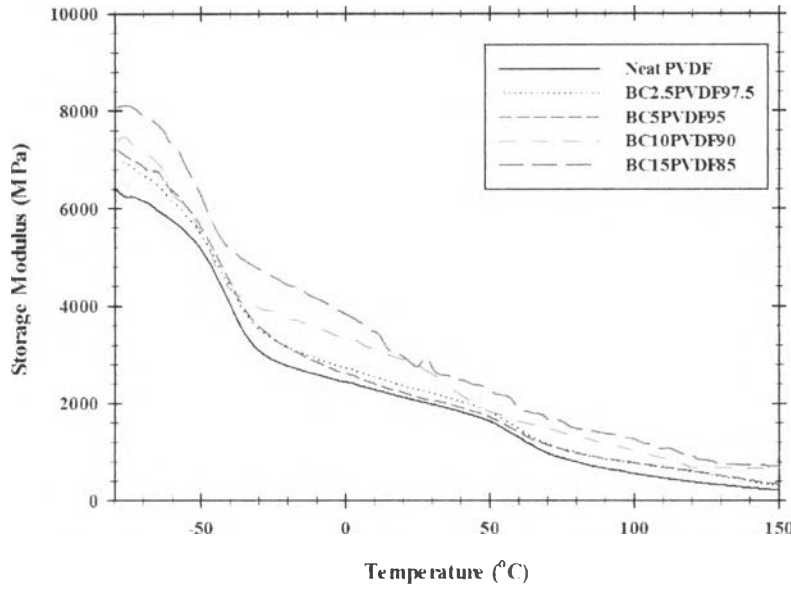

Figure 4.16 Storage tensile modulus, E' vs temperature of various amounts of BC in BC/PVDF blend films compared to neat PVDF.

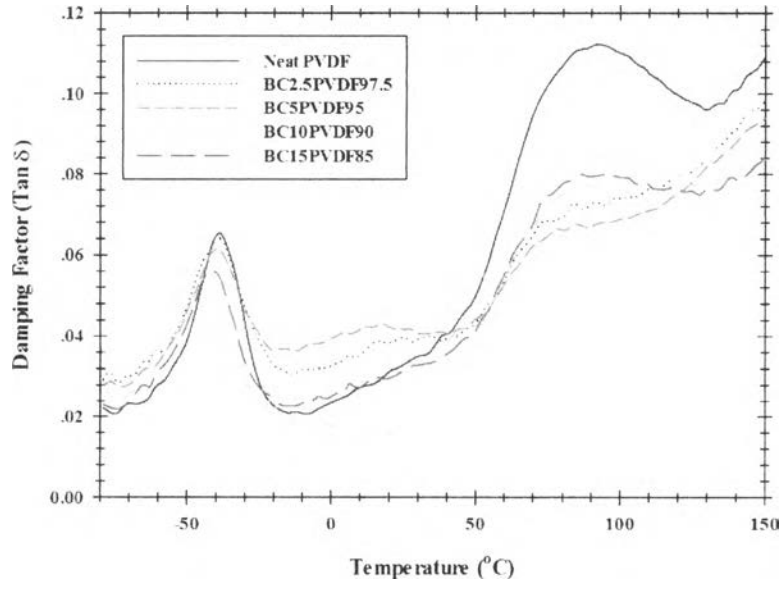

Figure 4.17 Damping factor (E"/E') vs temperature of various amounts of BC in BC/PVDF blend films compared to neat PVDF.

Table 4.3 Summary of transition temperature and storage modulus of BC/PVDF blend films at different composition from DMA technique

Sample	Transition temperature (°C)			storage modulus, E' (Mpa)		
	β	β'	α	-50 °C	0 °C	50 °C
Neat PVDF	-38.7	20.0	91.6	5108	2456	1578
BC2.5PVDF97.5	-38.6	25.2	91.9	5404	2757	1769
BC5PVDF95	-38.6	17.2	86.4	5549	2639	1663
BC10PVDF90	-41.2	23.9	104.0	6072	3607	1794
BC15PVDF85	-48.6	32.5	100.4	6489	4210	2191

4.4.2.6 Optical Properties of BC/PVDF Blend Films

The blend films' appearances are shown in Fig. 4.18, it was found that the films appearances become more opaque with the increasing of BC weight percentage, this optical result can be confirmed by Figure 4.19 which shows UV/Vis spectra of the neat PVDF and BC/PVDF blend films. Neat PVDF has 80-90% transmittance in the visible light region (400-750 nm), but when adding BC, the transmittance tends to decrease, which means BC exhibits the opacity property. It is due to the formation of a network structure in the BC. It can be suggested that with high amount of BC, may segregate from the blend to form a micro-sized aggregation which can be observed in the visible light region.

Figure 4.18 Sample appearances of BC/PVDF blend films compared with neat PVDF.

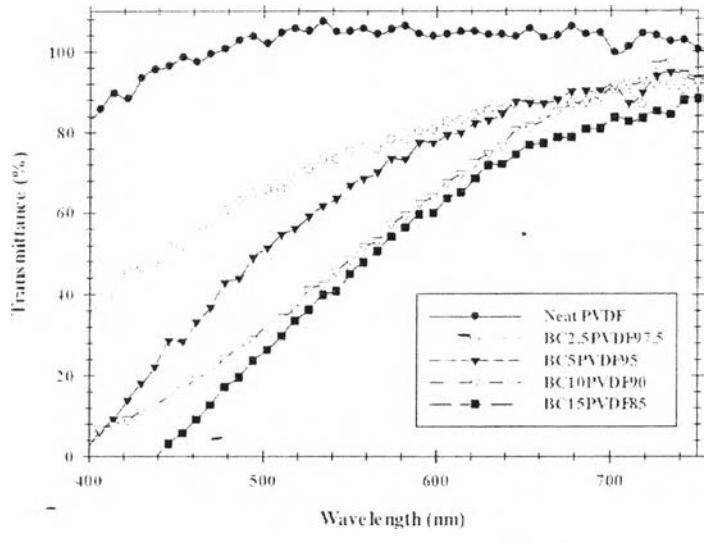

Figure 4.19 UV/Vis spectra of BC/PVDF blend films compared with neat PVDF.

4.4.2.7 Dielectric Properties of BC/PVDF Blend Films

The dielectric constant related to piezoelectric properties via the equation "$d_{ij} = \varepsilon_{ii}g_{ij}$" , where d_{ij} is stress piezoelectric coefficient, ε_{ii} is the permittivity of the material and g_{ij} is strain piezoelectric coefficient. This equation shows that the dielectric property is a basis property for piezoelectric materials. In this part, the effect of frequency, temperature and BC content on dielectric behavior of BC/PVDF blend films and neat PVDF were discussed.

Figure 4.20 exhibits the frequency and temperature dependence on dielectric constant of the BC/PVDF blend films with neat PVDF provided for comparison. At constant frequency with high temperature, the dielectric constant tended to be high due to PVDF chains can be free to vibrate, move and reorient which allow them to keep up with the changing electric field. When the successful orientation was obtained, the dielectric constant became constant. With lower temperature, the segmental motion of the chain is practically frozen when the temperature was much lower than dynamic T_g which cause the lower dielectric constant (Ahmad, 2012).

The dielectric constant on frequency dependence was found in the Figure 4.18. At low frequency, the dipoles in polymeric chain had sufficient time

to align with the electrical field direction causing to the higher dielectric constant. With higher frequency, the dipoles had short time to align with the electrical field direction, so the lower dielectric constant can be detected. It can be concluded that the dielectric behaviors of neat PVDF strongly depend on the variation of frequency and temperature.

From Figure 4.20 the dielectric constant and dissipation factor was at 3-16 and 0.02-0.40, respectively at wide range of temperature and 10 MHz, 100 MHZ and 1 GHz. Figure 4.22 shows dielectric constant a) and dissipation factor b) of BC/PVDF blend films compared to neat PVDF as a function of frequency at 20 °C. Compared to neat PVDF, blending with higher 5 wt% of BC exhibited significantly higher dielectric constant. This increasing occurred due to the interfacial polarization between the hydroxyl group in the BC chain and fluorine atom in PVDF chain, higher amount of polar hydroxyl group in BC, and the higher amount of β phase. However, higher amounts of BC were incorporated, more free space occurred from repulsive force between the hydroxyl groups, and it consequently decreased the polarization, resulted in decreasing of increasing on the dissipation factor which was observed at the BC content higher than 5 wt%. Moreover, a higher content of BC in the blend caused higher water content, which increased the loss of the blend films due to lower stability of the PVDF structure and a higher dissipation factor from the water. The dielectric constant on frequency dependence can be also explained as mentioned earlier.

The dielectric relaxation mechanism of neat PVDF and its blend films can be observed in Figure 4.21, it was found that there's only one relaxation mechanism appeared which was referred to the dynamic glass transition temperature (T_g) or the β relaxation that can be obtained by the dielectric response at very low frequency (Rao *et al.*, 2002). With the increasing of frequency (10 MHz to 100 MHz), this relaxation peak shifted to higher temperature (20 °C to 50 °C) because polymeric chains in amorphous region has not enough energy to relax due to the very short time to store the energy, so the higher energy was needed for the chains to vibrate and reorient along the electrical field. For the BC/PVDF blend films,

there's only one relaxation mechanism, which means that the incorporation of BC didn't have the effect on the relaxation behavior of the blend films.

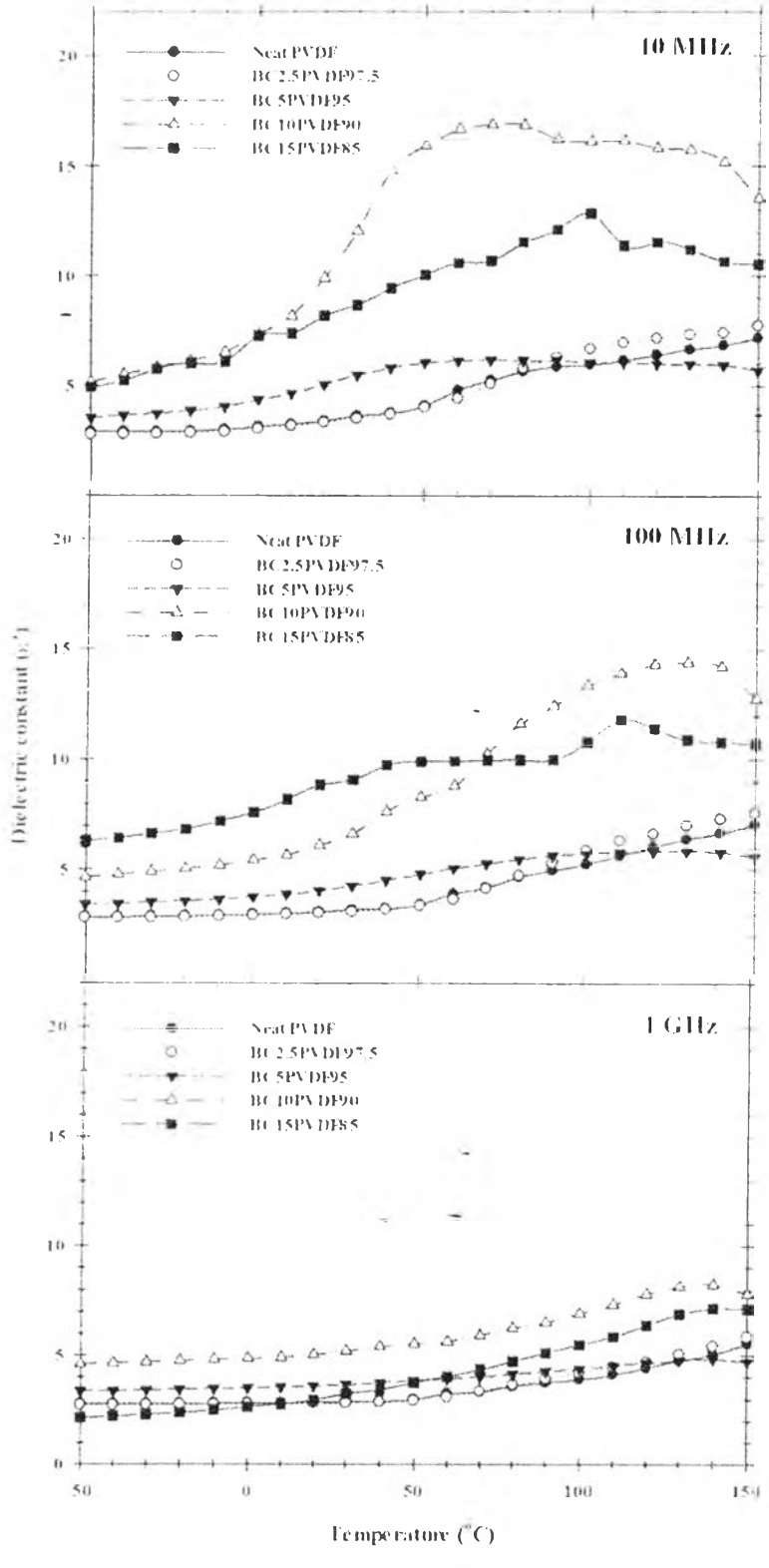

Figure 4.20 Dielectric constant of BC/PVDF blend films compared with neat PVDF at temperature -50 °C – 150 °C and 10 MHz, 100 MHz and 1 GHz.

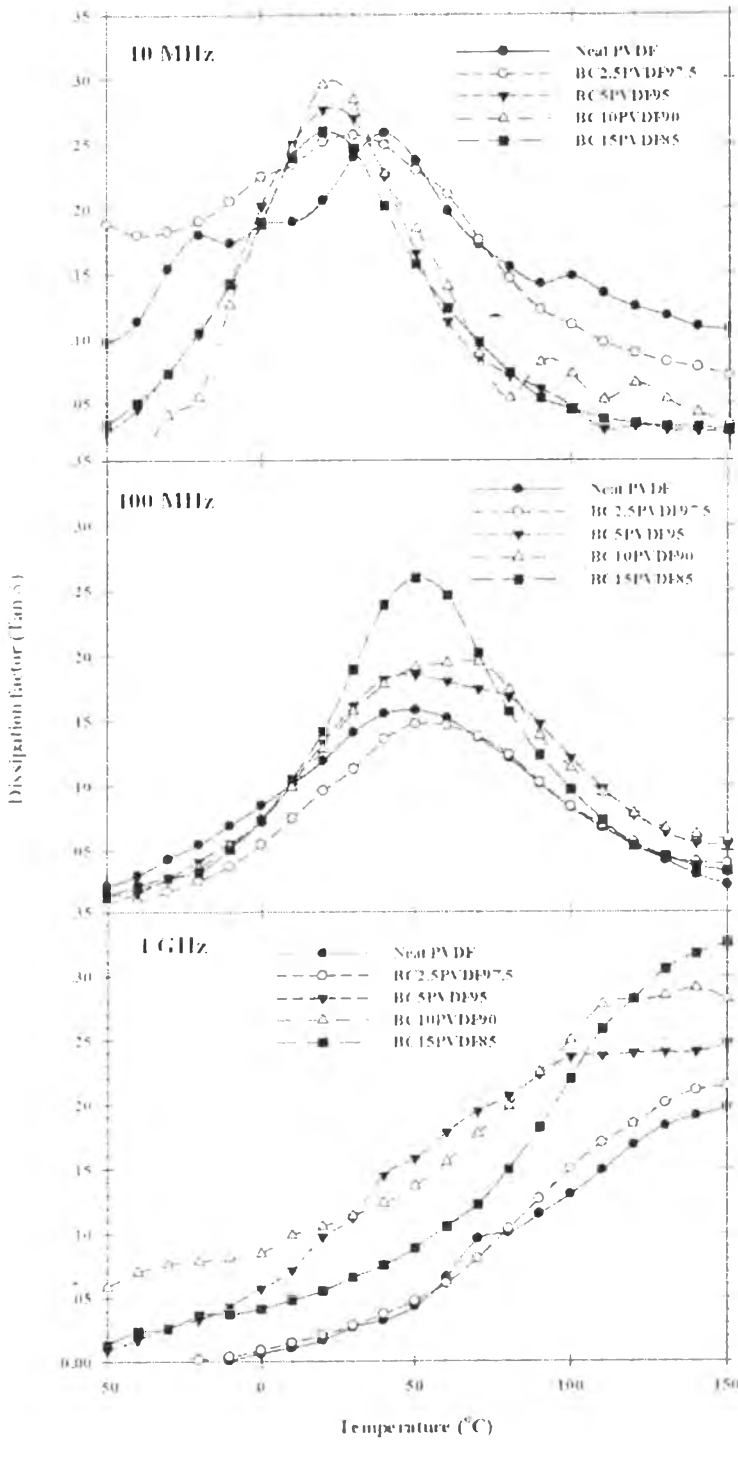

Figure 4.21 Dissipation factor of BC/PVDF blend films compared with neat PVDF at temperature -50 °C – 150 °C and 10 MHz, 100 MHz and 1 GHz.

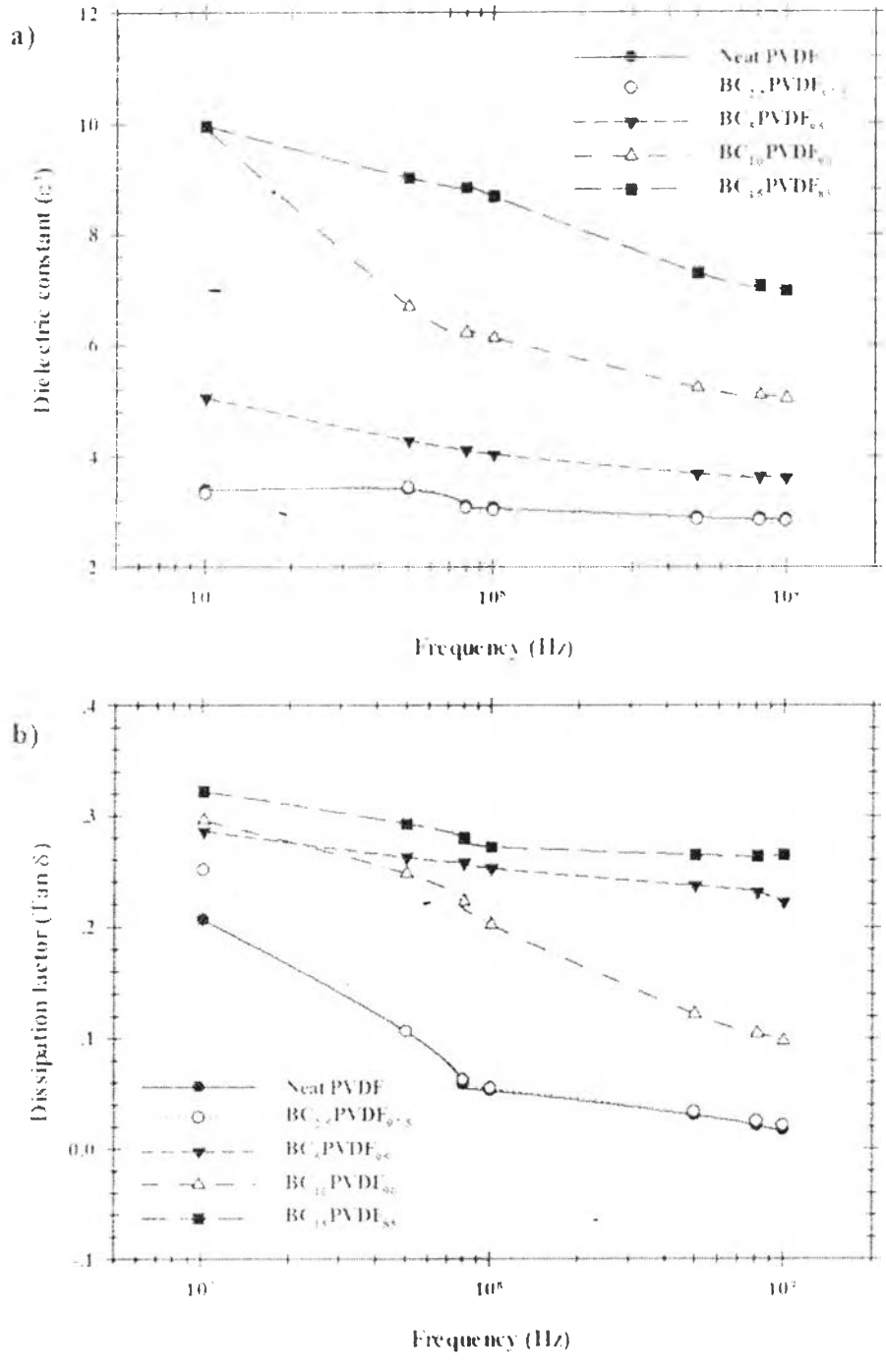

Figure 4.22 Dielectric constant a) and dissipation factor b) of BC/PVDF blend films compared with neat PVDF as a function of frequency at 20 °C.

4.5 Conclusion

Bacterial cellulose (BC) was blended with poly(vinylidene fluoride) (PVDF) by firstly solution casting method using dimethylformamide (DMF) as solvent. Then these casted blend films were further hot-compressed to obtain transparent and smooth surface free. The TEM nanographs indicated that BC has nano-scale diameter forming a network structure which yield the high surface area causing better physical attraction with PVDF surface. In addition, there was also the chemical attraction between hydroxyl group in BC structure and fluorine atom in PVDF chain. These interactions can be observed from the thermal stability. There were slightly increase of T_m and T_d of blend films. Storage modulus of the blend films was higher than neat PVDF significantly (at least 17%) at wide range of temperature. The results also show that there were the mixed phases of β and α-phase crystallinity. The partially interactions between the interface of BC and PVDF yield to enhance of dielectric properties. However, for the optical property, the incorporated of BC decreased the percentage of transmittance in all visible light range. The 2.5wt% of BC was chosen to further study the effect of silver nanoparticles on the relate properties with basis of piezoelectric touch sensor due to highest percentage of transmittance compare to other compositions, moderate storage modulus, moderate dielectric constant and lowest dissipation factor at any temperature and frequency.

4.6 Acknowledgement

The authors would like to sincerely thank the financial support from the Thailand Government Research Budget (contract number GRB_BSS_66_56_63_08), and the 90th Anniversary Chulalongkorn Fund (Ratchadaphiseksomphot Endowment Fund). We also appreciate the Solvay (Thailand) Co., Ltd. for material support.

4.7 References

Ahmad, Z. (2012) Polymeric Dielectric Material. Intech Open Access

Chae, D.W. and Hong, S. M. (2010) Dynamic crystallization behavior, morphology and physical properties of highly concentrated poly(vinylidene fluoride)/silver nanocomposites. Journal of Polymer Science: Part B: Polymer Physics, 48(22), 2379-2385.

Chang, W.Y., Fang, T.H., Liu, S.Y., and Lin, Y.C. (2008) Phase transformation and thermomechanical characteristics of stretched polyvinylidene fluoride. Materials Science and Engineering A, 480, 477-482.

Czaja, W., Romanovicz, D., and Malcom Brown, J.R. (2004) Structural investigations of microbial cellulose produced in stationary and agitated culture. Cellulose, 11(3-4), 403-411.

Dahan, R.M., Ismail, S.I., Latif, F., Sarip, M.N., Wahid, M.H., and Arshad, A.N. (2012) Dielectric properties of collagen on plasma modified polyvinylidene fluoride. Journal of Applied Sciences, 9(5), 694.

Fukada, E. and Furukawa, T. (1981) Piezoelectricity and ferroelectricity in polyvinylidene fluoride. Ultrasonics, 19(1), 31-39.

Halib, N., Iqbal, M.C., Amin, M., and Ahmad, I. (2012) Physicochemical properties and characterization of Nata de Coco from local food industries as a source of celluose. Sains Malaysiana, 42(2), 205-211.

Harrison, J.S. and Ounaies, Z. (2001) Piezoelectric Polymers. ICASE, 211422. Virginia, Natrional Aeronautics and Spcae Administration, Langley Research Center, Hampton, Virginia.

Maneerung, T., Tokura, S., and Rujiravanit, R. (2008) Impregnation of silver nanoparticles into bacterial cellulose for antimicrobial wound dressing. Carbohydrate Polymers, 72(1), 43-51.

Marcovich, N.E., Auad, M.L., Bellesi, N.E., Nutt, S.R., and Aranguren, M.I. (2006) Cellulose Micro/Nanocrystals Reinforced Polyurethane. Journal of Materials Research, 21(4), 870-881.

O-Rak, K. (2013) Poly(vinylidene fluoride)/bacterial cellulose nanocomposite films for touch sensor applications. M.S. Thesis, The Petroleum and Petrochemical College, Chulalongkorn University, Bangkok, Thailand.

O-Rak, K., Phakdeepataraphan, E., Bunnak, N., Ummartyotin, S., Sain, M., and Manuspiya, H. (2014) Development of bacterial cellulose and poly(vinylidene fluoride) binary blend system: Structure and properties. Chemical Engineering Journal, 237, 396-402.

Patro, T.U., Mhalgi, M.V., Khakhar, D.V., and Misra, A. (2008) Studies on poly(vinylidene fluoride)–clay nanocomposites: Effect of different clay modifiers. Polymer, 49(16), 3486-3499.

Rao, V., Ashokan, P.V., and Amar, J.V. (2002) Studies on dielectric relaxation and AC conductivity of cellulose acetate hydrogen - phthalate-poly(vinyl pyrrolidone) blend. Journal of Applied Polymer Science, 86(7), 1702-1708.

Ratanakamnuana, U., Atong, D., and Aht-Ong, D. (2012) Cellulose esters from waste cotton fabric via conventional and microwave heating. Carbohydrate Polymers, 87(1), 84-94.

Rekik, H., Ghallabi, Z., Royqud, I., Arous, M., Seytre, G., Boiteux, G., and Kallel, A. (2013) Dielectric relaxation behavior in semi-crystalline polyvinylidene fluoride (PVDF)/TiO_2 nanocomposites. Composites: Part B, 45(1), 1199-1206.

Salimi, A. and Yousefi, A.A. (2003) FTIR studies of β-phase crystal formation in stretched PVDF films. Polymer Testing, 22(6), 699-704.

Shah, N., Ul-Islam, M., Khattak, W.A., and Park, J.K. (2013) Overview of bacterial cellulose composites: A multipurpose advanced material. Carbohydrate Polymers, 98(2), 1585-1598.

Shin, Y.H., Cho, C.K., and Kim, H.K. (2013) Resistance and transparency tunable Ag-inserted transparent InZnO films for capacitive touch screen panels. Thin Solid Films, 548, 641-645.

Tang, C. and Liu, H. (2008) Cellulose nanofiber reinforced poly(vinyl alcohol) composite film with high visible light transmittance. Composites: Part A, 39(10), 1638-1643.

Ummartyotin, S., Juntaro, J., Sain, M., and Manuspiya, H. (2012) Development of transparent bacterial cellulose nanocomposite film as substrate for flexible organic light emitting diode (OLED) display. Industrial Crops and Products, 35(1), 92-97.

Wu, J., Zheng, Y., Song, W., Luan, J., Wen, X., Wu, Z., Chen, X., Wang, Q., and Guo, S. (2014) In situ synthesis of silver-nanoparticles/bacterial cellulose composites for slow-released antimicrobial wound dressing. Carbohydrate Polymers, 102, 762-771.

Zhang, X., Feng, J., Liu, X., and Zhu, K. (2012) Preparation and characterization of regenerated cellulose/poly(vinylidene fluoride) (PVDF) blend films. Carbohydrate Polymers, 89(1), 67-71.